Transactions of the Royal Society of Edinburgh: Earth Sciences, **95**, 297–307, 2004

Late Archaean Kenogamissi complex, Abitibi Subprovince, Ontario, Canada: doming, folding and deformation-assisted melt remobilisation during syntectonic batholith emplacement

Keith Benn

ABSTRACT: The Kenogamissi complex represents a large exposure of folded Late Archaean crystalline crust exposed within the Abitibi Subprovince, Ontario, Canada. It is composed of an heterogeneous amphibolite-grade orthogneiss unit, and several generations of batholiths and plutons of tonalite, granodiorite and granite composition. Together, the various units represent granitic magmatism during the period from 2740 Ma to 2660 Ma. Structural mapping and petrographic studies were focused on the orthogneiss unit (2723 Ma), on the newly defined Roblin tonalite-granodiorite batholith (ca. 2713 Ma) and on the highly strained metavolcanic rocks within the deformation aureole that surrounds the Kenogamissi complex. Structural analysis indicates that the Kenogamissi complex was emplaced into the greenstones as a dome that caused severe flattening and recumbent F2 refolding of earlier F1 folds in the deformation aureole. Doming is interpreted to be caused by the emplacement and inflation of tonalite-granodiorite batholiths, such as the Roblin Batholith, into the actively folding Swayze greenstone belt. Continued regional folding resulted in F3 refolding of F1 and F2 in the deformation aureole. Continued regional folding also deformed and folded the Kenogamissi complex and resulted in further uplift and emplacement of the complex into the greenstone belt. The early-formed magmatic foliation and compositional layering in the Roblin Batholith were folded by F3 while the batholith was still a crystal mush, and an F3 axial-surface magmatic foliation was locally formed. Folding of the partially molten Roblin Batholith also resulted in the remobilisation of fractionated liquids into shear zones which formed on the limbs of the F3 magmatic folds. Similar structures are present in the orthogneiss unit and are interpreted to represent remobilisation of melts which intruded the orthogneiss at the time of emplacement of the Roblin Batholith. The formation of the dykes on sheared fold limbs may be attributed to increased dilatancy during localised shearing of the crystal mush. Deformation-assisted remobilisation and extraction of fractionated liquids, and the possible transport of the fractionated liquids to higher levels in the crystallising Roblin Batholith, may have played a role in its magmatic differentiation.

KEY WORDS: Granite, melt extraction, pluton emplacement, Swayze greenstone belt.

The Late Archaean Abitibi Subprovince is one of the largest and most studied granite-greenstone terranes in the Superior Province of the Canadian Shield, and indeed, on Earth. It includes several greenstone belts, the largest of which are the mineral-rich Abitibi belt and the Swayze belt, which is situated in the SW part of the Abitibi Subprovince. In the Ontario (western) portion of the Abitibi Subprovince (Fig. 1), the supracrustal rocks have been lithologically and, to a lesser extent, structurally mapped in some detail. The mapping, together with petrological and geochronological studies have provided a fairly robust stratigraphic framework for the supracrustal rocks (Ayer *et al.* 2002a). Large batholiths within the Abitibi Subprovince have received less attention, especially from a structural point of view. The present paper describes new structural data from and interpretations of the Kenogamissi complex, a large crystalline complex in the western Abitibi Subprovince.

The Kenogamissi complex includes a suite of plutons of tonalite, granodiorite and granite compositions which represent magmatism spanning some 80 Ma, from 2740 Ma to 2660 Ma. Some of the plutonic rocks have been strongly deformed and locally transformed to orthogneiss of diorite and tonalite compositions, whereas other plutons preserve pristine igneous textures. In this paper, attention is focused on some key results of mapping and petrographic study of the orthogneiss, and a large, newly defined tonalite-granodiorite batholith, the Roblin Batholith, which together represent a large portion of the Kenogamissi complex.

In the course of mapping, it was demonstrated that the Kenogamissi complex represents a refolded dome emplaced into previously folded greenstones of the upper crust. The host greenstone belt and the Kenogamissi complex were then folded together. Emplacement of the Roblin Batholith occurred during doming and folding. The results and interpretations presented here suggest that the Kenogamissi dome was emplaced during the single long-lived, E–W upright folding event that deformed the entire Abitibi Subprovince, ca. 2715 Ma through 2700 Ma.

The Roblin Batholith was folded while it remained a crystallising mush, resulting in magmatic folds, in local overprinting of early-formed magmatic structures and in remobilisation of fractionated melts within the batholith. Magma remobilisation structures are documented within the orthogneiss and also within the Roblin Batholith, and it is suggested that magmatic differentiation of the batholith may have been enhanced by the regional deformation and folding.

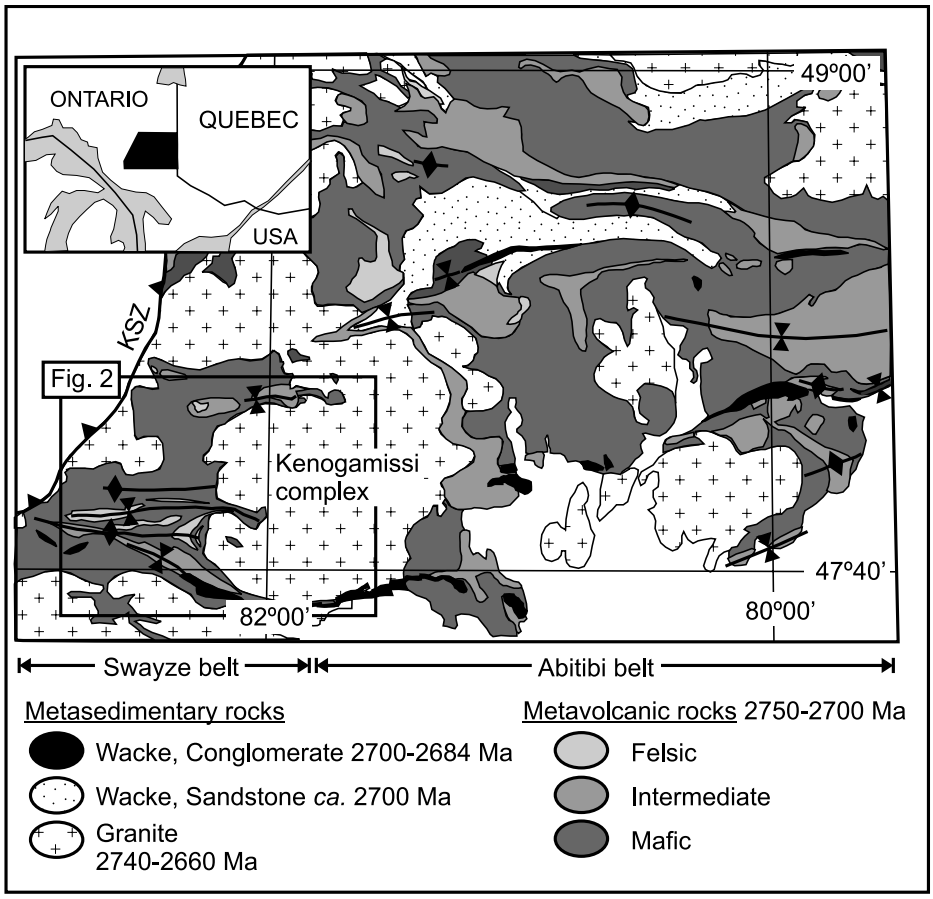

Figure 1 Map of the Abitibi Subprovince in Ontario, Canada, compiled from 1:100 000-scale maps published by the Ontario Geological Survey.

1. Geological setting

The Late Archaean Abitibi Subprovince is situated within the south-eastern portion of the Superior Province, in the Canadian Shield. In Ontario, the Abitibi Subprovince comprises several greenstone belts, of which the Abitibi greenstone belt (Fig. 1) is the largest and the most extensively studied. The smaller Swayze greenstone belt is situated in the western part of the Abitibi Subprovince (Figs 1 & 2), where its western limit corresponds to the Kapuskasing structure, a Proterozoic uplift of Archaean high-grade metamorphic rocks corresponding to a crustal-scale thrust or flower structure (Percival 1988; Nitescu & Halls 2002). The Kenogamissi complex, a large crystalline complex composed of multiple plutons of distinctly different ages, straddles the boundary between the Abitibi and Swayze greenstone belts (Fig. 1).

On its western and southern borders, the Kenogamissi complex crops out within greenschist-grade mafic to felsic metavolcanic rocks of the Swayze greenstone belt (Fig. 2). The metavolcanic units which host the Kenogamissi complex were deposited between approximately 2750 and 2705 Ma (Fig. 2; U-Pb zircon geochronological data reported in Heather 1999). The Swayze and Abitibi greenstone belts are deformed by one generation of upright, moderately doubly-plunging, E–W-trending regional-scale folds. In the region depicted in Figure 2, the older metavolcanic units, the Chester and Marion Groups, crop out in the south, whereas the younger metavolcanic units, the Trailbreaker Group, and the Newton and Brett Lake Formations, crop out in the north, suggesting that, viewed in profile, the regional-scale folds define an asymmetrical pattern with southward vergence.

2. Rock units and geochronology

The main rock types of the Kenogamissi complex are discussed with reference to Figure 2, which was compiled and modified from existing 1:50 000-scale maps (Heather 1999) with contacts between plutonic units added or modified according to field mapping by the present author. The plutonic units are presented in relative chronological age (oldest to youngest) based on cross-cutting relationships documented during mapping and on published single-zircon geochronological data (Heather 1999; Ayer *et al.* 2002b).

2.1. Amphibole-biotite tonalite

The amphibole-biotite tonalite has an apparent crystallisation age constrained by U-Pb zircon dates of $2741 \pm 2{\cdot}5$ to $2746 \pm 1{\cdot}3$ Ma which were obtained for samples from the south-western lobe of the Kenogamissi complex. The dates for the amphibole-biotite tonalite unit are comparable to the oldest exposed volcanic units of the Swayze and Abitibi greenstone belts. Tonalite plutons of similar ages elsewhere in the Abitibi Subprovince are interpreted to represent magma chambers associated with the older metavolcanic units (Sutcliffe *et al.* 1993). That interpretation is adopted here for the amphibole-biotite tonalite unit of the Kenogamissi complex. The unit is compositionally homogeneous and it has undergone partial dynamic recrystallisation under amphibolite-grade conditions, although igneous textures are locally preserved (Becker & Benn 2003). As a result, the rock is generally well foliated.

https://doi.org/10.1017/S0263593300001085 Published online by Cambridge University Press

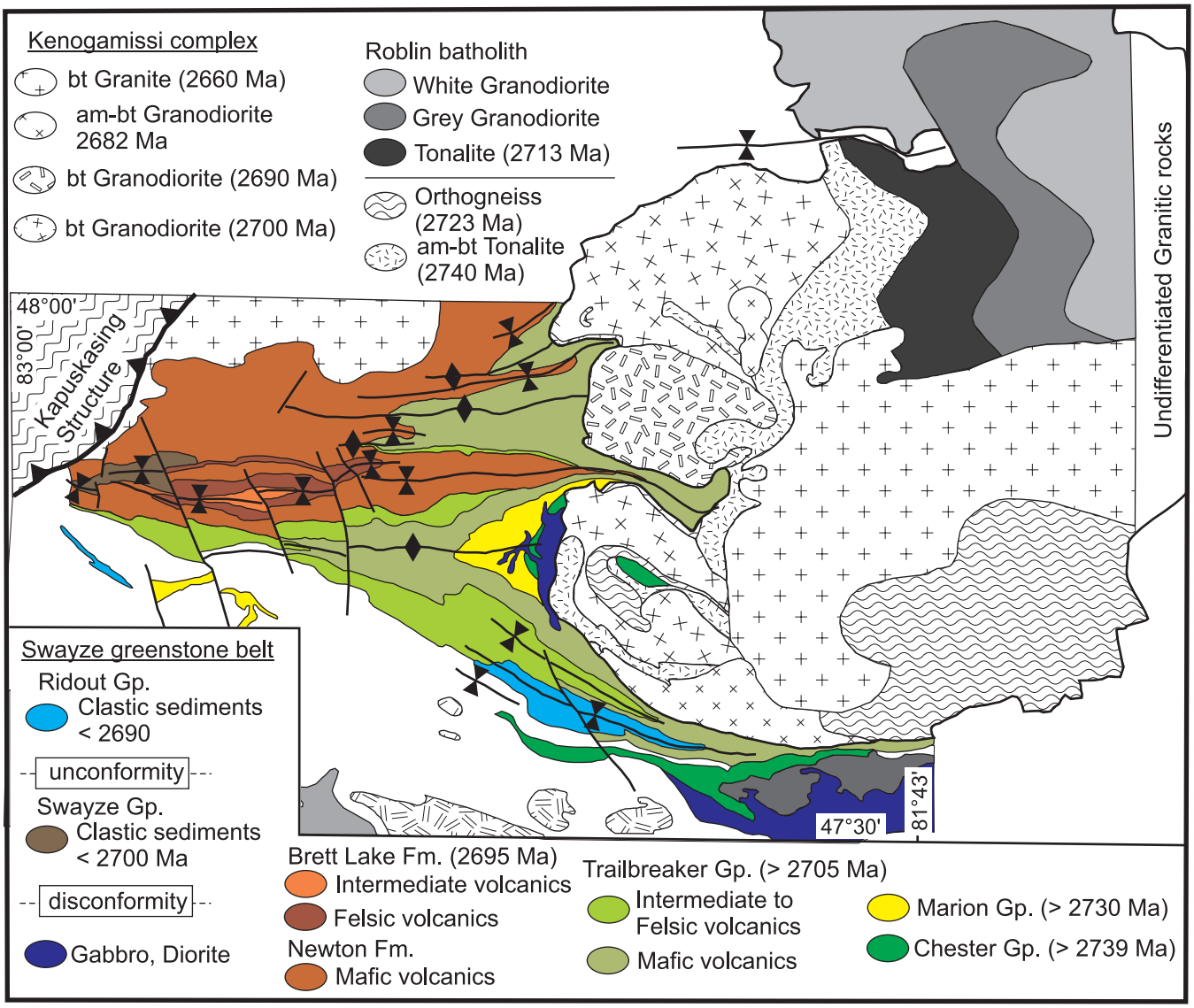

Figure 2 Geological map of the Swayze greenstone belt, and the central and western parts of the Kenogamissi complex (location indicated in Fig. 1). Compiled from 1:50 000-scale maps, and geochronological data published in Heather (1999) and Ayer *et al.* (2002b), with the internal contacts of the Kenogamissi complex modified according to mapping by the present author.

2.2. Orthogneiss

The orthogneiss unit is compositionally heterogeneous. It is mainly composed of medium-grained, mesocratic amphibole-biotite tonalite and finer grained biotite leucotonalite, with a lesser but significant proportion represented by fine- to medium-grained amphibolite, diorite, melanocratic tonalite and biotite granodiorite. Cross-cutting and xenolith relationships indicate the orthogneiss is composed of multiple generations of intrusions, most of which have been isoclinally folded (Fig. 3A).

Microprobe analyses (this author's unpublished data) revealed the amphiboles of the mesocratic tonalite to be hastingsite to hastingsitic ferro-hornblende in composition. The mesocratic tonalite component of the orthogneiss commonly contains mafic inclusions of melanotonalite to diorite composition (seen above the compass in Fig. 3B) which are interpreted to represent boudinaged xenoliths. The characteristic granoblastic microstructures and quartz ribbons (Fig. 4A) record dynamic recrystallisation and fabric development under the amphibolite-grade metamorphic conditions which accompanied isoclinal folding.

One U-Pb zircon date of 2723 Ma has been published for an outcrop of orthogneiss located within a few tens of metres of the one shown in Figure 3A. The orthogneiss is quite heterogeneous in composition, and may include components with different ages. Further geochronological study will be required to determine the ages of the different components.

2.3. The Roblin Batholith

Three easily distinguishable and mappable units are grouped together into a newly defined batholith, here named the Roblin Batholith (Fig. 2). The structurally lowest unit of the batholith is composed of tonalite that grades upward into grey and white granodiorite units.

The tonalite unit is typically strongly foliated and contains biotite ± dark green amphibole as ferrosilicate minerals. A U-Pb zircon date for a compositionally homogeneous outcrop of this unit yielded 2713 ± 3 Ma, which is interpreted to represent the crystallisation age.

The grey granodiorite unit overlies the tonalite. No intrusive relationships between this unit and the tonalite unit were documented in the field, and it is interpreted that the two units are gradational one to the other. Typically, amphibole is absent from this unit, which is characterised by large K-feldspar phenocrysts which, along with biotite crystals,

https://doi.org/10.1017/S0263593300001085 Published online by Cambridge University Press

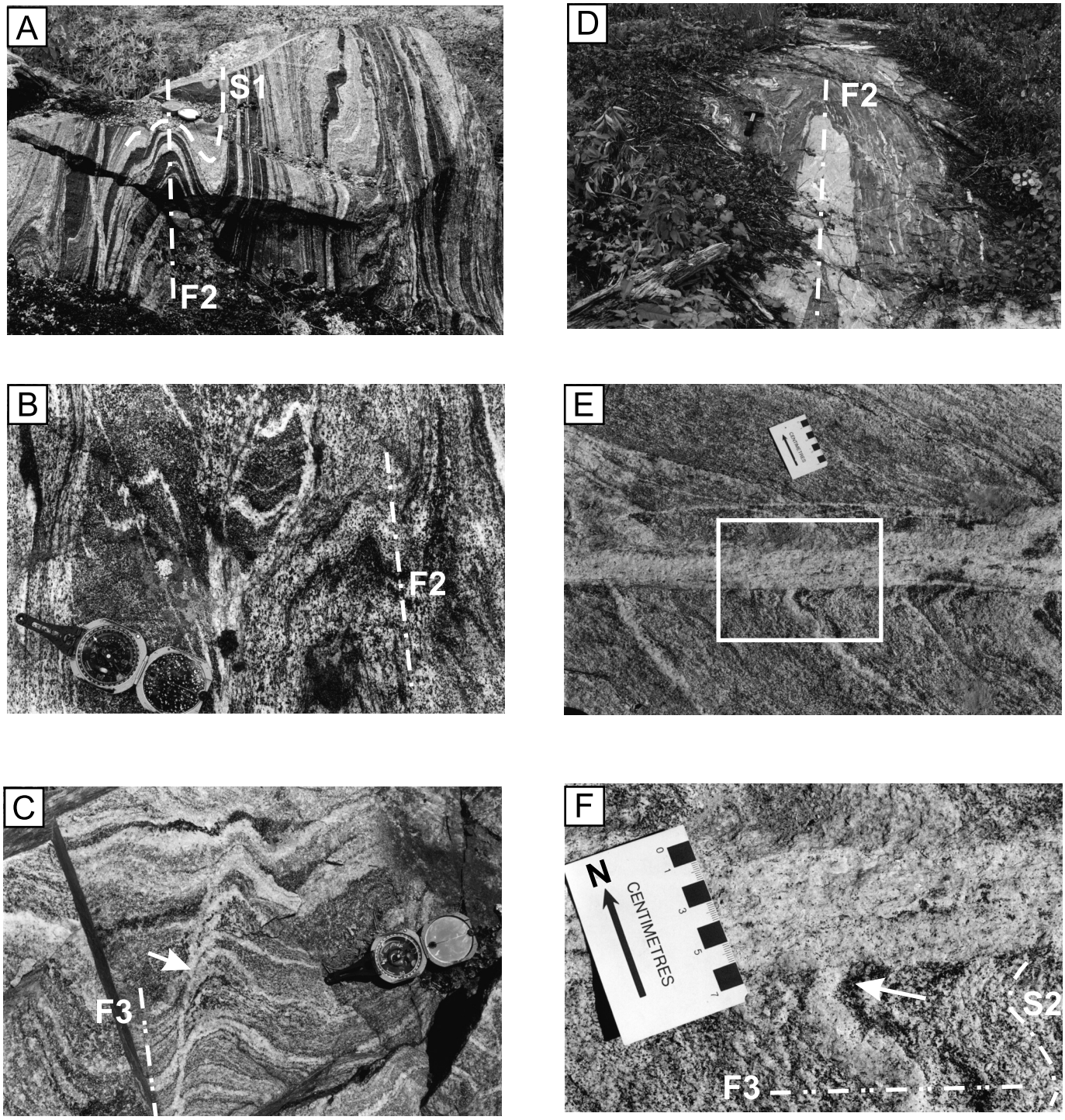

Figure 3 (A) F2 isoclinal folds of S1 and of the compositional layering in the orthogneiss unit. The F2 folds at that locality have been steepened by F3 folding. Compass for scale. (B) Boudins of melanocratic tonalite (darker) containing F2-folded leucocratic veins, hosted within a medium-grained tonalite facies that has also been deformed by F2. Compass for scale. (C) Compositional banding in the orthogneiss unit folded by F3. The arrow indicates a leucocratic dyke on the limb of an F3 fold that cross-cuts the banding and the S2 foliation, and that terminates in a banding-parallel sill. The outcrop surface is vertical. Compass for scale. (D) An F2-folded granodiorite dyke (light grey) that crops out within the deformation aureole of the Kenogamissi complex. The F2 fold has been steepened by F3 folding. Hammer for scale. (E) Leucocratic dyke emplaced on the sheared limb of an F3 fold in the tonalite unit of the Roblin Batholith. The rectangle shows the location of Figure 3F. (F) Detail of the dyke shown in Figure 3E, showing its contiguity with the S2 foliation-parallel leucocratic bands.

define the foliation. It is distinguished from the unit described next by the relative abundance of biotite (15–20% modal abundance), which is responsible for the grey colour of the rock in outcrop.

The white granodiorite (to granite) unit is distinguished from the previous one by its white colour in outcrop because of its more leucocratic composition. Biotite represents only about 5–8% modal percentage of the rock and it contains abundant K-feldspar phenocrysts. Blocks of the grey granodiorite unit are indentified within this unit. The magmatic foliation within the blocks is locally concordant to the magmatic foliation in the host white granodiorite, but in other cases, it is discordant. The blocks are interpreted to represent autoclaves of the earlier crystallised grey granodiorite components of the batholith.

https://doi.org/10.1017/S0263593300001085 Published online by Cambridge University Press

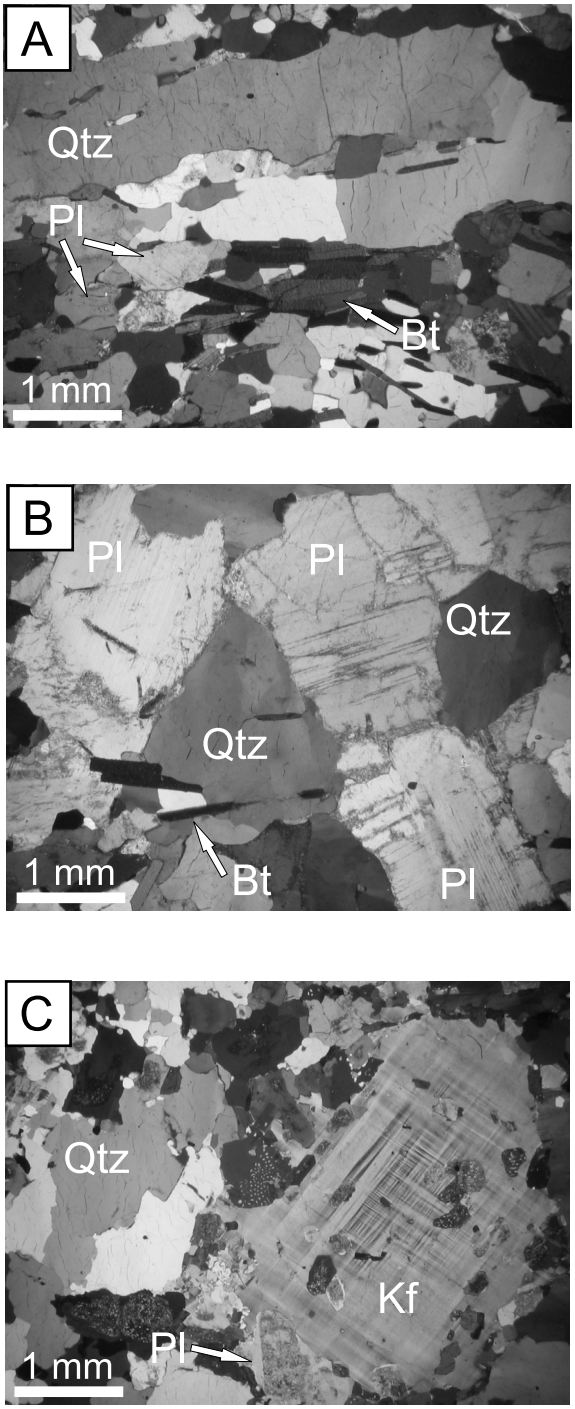

Figure 4 Photomicrographs of textures in three rock units: (A) Tonalite orthogneiss with a fine-grained dynamically recrystallised quartzo-feldspathic matrix and highly elongate quartz ribbons; (B) Tonalite unit of the Roblin Batholith. The sample has a well-preserved igneous texture with subhedral to euhedral plagioclase crystals and interstital quartz grains which have slightly undulose extinction; (C) White granodiorite unit of the Roblin Batholith. The igneous texture is indicated by the presence of subhedral to euhedral K-feldspar phenocrysts and plagioclase crystals, and coarse-grained interstitial quartz that shows evidence of minor subgrain development. Abbreviations: (Qtz) quartz; (Pl) plagioclase; (Bt) biotite; and (Kf) K-feldspar.

2.4. Biotite granodiorites

Two biotite granodiorite units are indentified within the Kenogamissi complex (Fig. 2) based on geochronological data and textural observations. Samples of the older unit yielded zircon dates within the range 2700 ± 2 Ma (Ayer *et al*. 2002b) from outcrops in the south-western lobe of the Kenogamissi complex. The younger of the biotite granodiorite units is considered to belong to a suite of plutons which yielded zircon dates of ca. 2690 Ma (Heather 1999). The two units may be distinguished in the field by the common presence of biotite-rich enclaves in the younger one (Heather 1999). Both biotite granodiorite units are texturally distinct from the granodiorites of the Roblin Batholith in that they are devoid of phenocrysts.

2.5. Amphibole-biotite granodiorite

This unit crops out mainly along the southern margin of the Kenogamissi complex. It contains abundant phenocrysts of K-feldspar and it is easily distinguished from the other granodiorite units by the ubiquitous presence of dark green amphibole, and also by the common presence of subangular xenoliths or enclaves of amphibolitic material which are a few centimetres in size. A published U-Pb zircon date for the unit is 2682 ± 3 Ma (Heather 1999).

2.6. Biotite granite

The youngest intrusive unit in the study area is a fine- to medium-grained biotite granite, commonly associated with abundant coeval pegmatite. The rock is easily identified by its distinctive pink colour in outcrop and by its common association with pegmatite. Observations of cross-cutting relationships in the field show that this unit intruded all other plutonic units in the study area. It forms abundant dykes which occur in most outcrops, and a large map unit is defined (Fig. 2). A U-Pb zircon date for this unit is 2660 Ma.

3. Structural geology

In this section, the present author summarises the essential elements of the structural geology of the study area. The focus is on structures in the marginal greenstones which form a narrow (10^2 to 10^3 m) deformation aureole around the Kenogamissi complex, on metamorphic structures in the orthogneiss unit and on magmatic structures in the Roblin Batholith. Melt remobilisation structures in the orthogneiss and in the Roblin Batholith are also documented.

Figure 6A is a map of the Kenogamissi complex that includes representative measurements of structures in the orthogneiss and the Roblin Batholith. Figure 6B is a profile through the batholith along the line A′–B′ in Figure 6A. Figure 7 presents equal-area nets of structural measurements.

3.1. Structures in the marginal greenstones

The marginal greentones of the deformation aureole surrounding the Kenogamissi complex have been deformed by three generations of folds. Two of them can be neatly summarised with reference to the fold interference pattern in Figure 5A, which is a photograph of an horizontal outcrop surface. The outcrop is located in Figure 6B.

Figure 5A shows a type 3 refold interference pattern (Ramsay 1967) involving F1 and F2 folds (see also the inset in Fig. 6B). Both generations of folds, F1 and F2, have an associated axial planar foliation (S1 and S2, respectively).

The F2 folds in Figure 5A are in an upright orientation (the axial surfaces dip steeply) because of rotation by later E–W- to NW–SE-trending regional F3 folds (Fig. 6A) which are upright and gently to moderately doubly plunging. The upright F3 folds record the regional horizontal bulk N–S shortening that deformed the Abitibi Subprovince. Prior to F3 folding, the F2 folds must have been shallowly dipping (recumbent) such that they were refolded during the F3 bulk horizontal shortening event.

Refold interference patterns of type 3 require that the two generations of folds, in this case F1 and F2, have axial surfaces which were perpendicular (or nearly so) and fold axes which

https://doi.org/10.1017/S0263593300001085 Published online by Cambridge University Press

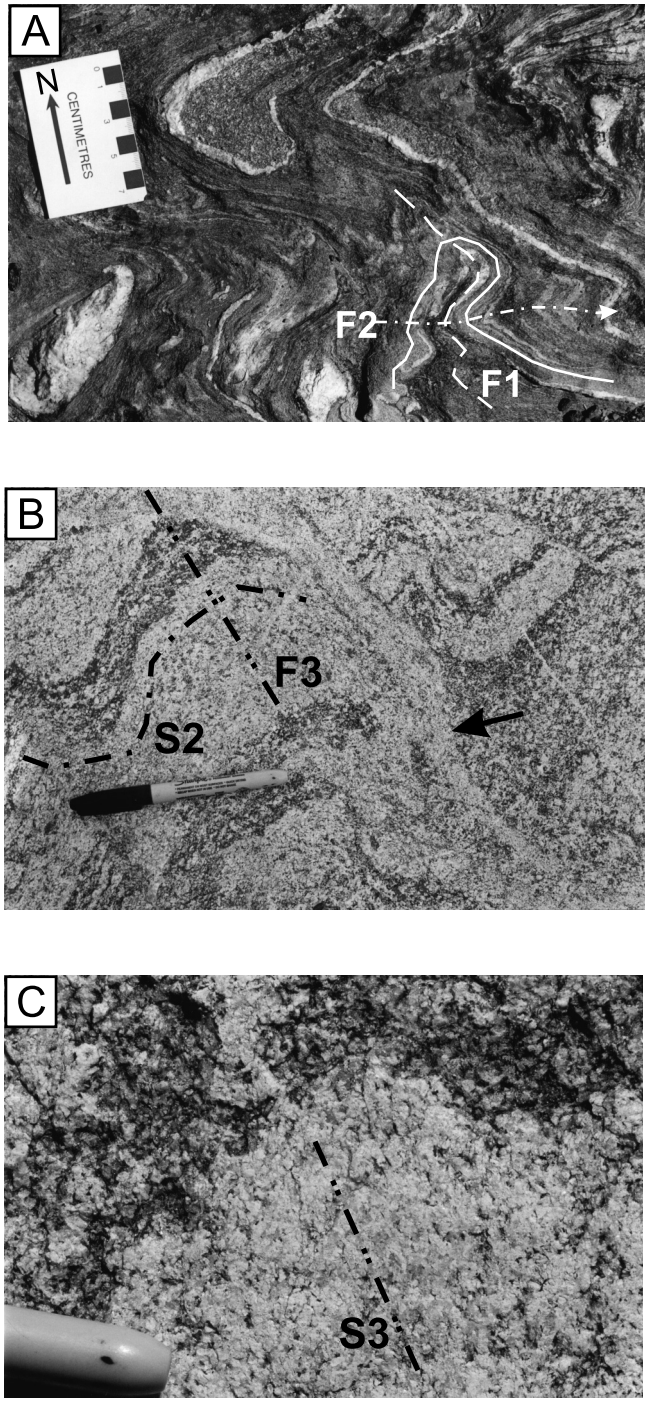

Figure 5 (A) Photograph of a horizontal greenstone outcrop surface in the deformation aureole of the Kenogamissi complex. See Figure 6B for the location. The type 3 fold interference pattern is caused by refolding of F1 folds by F2 folds. (B) F3 magmatic folds in an outcrop where the grey and white granodiorite units of the Roblin Batholith are interlayered. Note the leucocratic dyke (indicated by an arrow) within the sheared limb of an F3 fold. Pen for scale. (C) Detail of the contact between layers of grey and white granodiorite, in the hinge of an F3 magmatic fold in the granodiorites of the Roblin Batholith. The S3 foliation, defined by bt crystals, overprints the S2 foliation in the leucocratic layer. The pen tip provides the scale.

were parallel to oblique (Thiessen 1986). The type 3 refold pattern in Figure 5A requires that the axial surfaces of F1 folds were upright, perpendicular to originally recumbent axial surfaces of F2 folds. The type 3 pattern also requires that the F1 hinges were parallel to oblique to the F2 hinges. F2 folds are also documented in the orthogneiss unit (section 3.2; Fig. 7C).

3.2. Metamorphic structures in the orthogneiss

The orthogneiss unit is characterised by a penetrative gneissic banding and a parallel mineral foliation (Fig. 3A). The foliation is interpreted to represent an S1 fabric, as it is folded around the hinges of isoclinal F2 folds. It is interpreted to be correlative with the S1 foliation in the marginal greenstones. A mineral lineation, defined mainly by dark green prismatic amphibole, was measured in the S1 plane and it is interpreted to represent an L1 lineation.

The S1 foliation is folded into isoclinal F2 folds (Fig. 3A, B) which are commonly rootless. The constructed F2 fold axis, based on the distribution of S1 poles, suggests a NE–SW-trending and shallowly plunging fold axis (Fig. 7A). Dispersion of the S1 poles from the great circle in Figure 7A may be partly caused by later F3 folding. The L1 lineation orientations are quite scattered (Fig. 7B), presumably because of the subsequent F2 and F3 folding. The F2 fold hinges measured in the field define a NE–SW striking, vertical partial girdle caused by later F3 folding about a SE-trending axis (Fig. 7C). The distribution of the F2 fold hinges on a great circle (Fig. 7C) suggests that the axis of later F3 folding was roughly perpendicular to the F2 hinges.

In Figure 3 parts A and B, the axial surfaces of F2 folds have been tilted to an upright orientation by F3 folding. Many other outcrops have been mapped where the isoclinal F2 folds are in a recumbent orientation within hinge zones of the later F3 folds. The F2 folds in the orthogneiss unit are interpreted to have formed as recumbent folds which record intense flattening during the same event that caused F2 recumbent folding in the overlying marginal greenstones.

3.3. Magmatic structures in the Roblin Batholith

Igneous textures are well preserved in most outcrops of the three units of the Roblin Batholith. Petrographic study reveals the preservation of euhedral to subhedral biotite, plagioclase and K-feldspar crystals, and interstital quartz grains, the deformation of which is limited mainly to undulose extinction and minor subgrain development (Fig. 4B, C; cf. criteria for indentifying igneous fabrics in Bouchez *et al*. 1990; Paterson *et al*. 1989; Vernon 2000). Textural evidence for dynamic recrystallisation of quartz is observed in thin sections from some outcrops of the tonalite unit. The pervasive foliation that is present in all three units is interpreted to be of magmatic origin. It is defined by biotite and plagioclase crystals in the tonalite unit, and also by K-feldspar crystals in the grey and white granodiorite units. Near the mapped contact between the grey and white granodiorite units, compositional banding is also parallel to, and highlights, the foliation (Fig. 5B). This observation suggests an interlayering of the two units in a gradational transition zone between them.

The magmatic foliation in the Roblin Batholith is folded by one generation of upright folds, interpreted to be F3 (Fig. 5B, C), so the foliation must predate the F3 folds. Within the deformation aureole that surrounds the Kenogamissi complex, granodiorite dykes, thought to represent Roblin Batholith magmas, cross-cut the S1 foliation in the greenstones, are folded by F2 (Fig. 3D) and contain an S2 axial planar foliation, suggesting post-D1, pre- to syn-D2 emplacement of the Roblin Batholith. Based on these observations, the magmatic foliation in the Roblin Batholith is designated an S2 foliation.

The originally shallow dip angle of the S2 magmatic fabric is preserved in the hinge zones of the F3 folds, but in many outcrops, S2 has been rotated into steeper orientations (Fig. 7D). In the mapped area, measured F3 magmatic fold hinges trend to the southeast and have an average plunge angle of about 30° (Fig. 7E). The F3 folds of the magmatic fabric in

https://doi.org/10.1017/S0263593300001085 Published online by Cambridge University Press

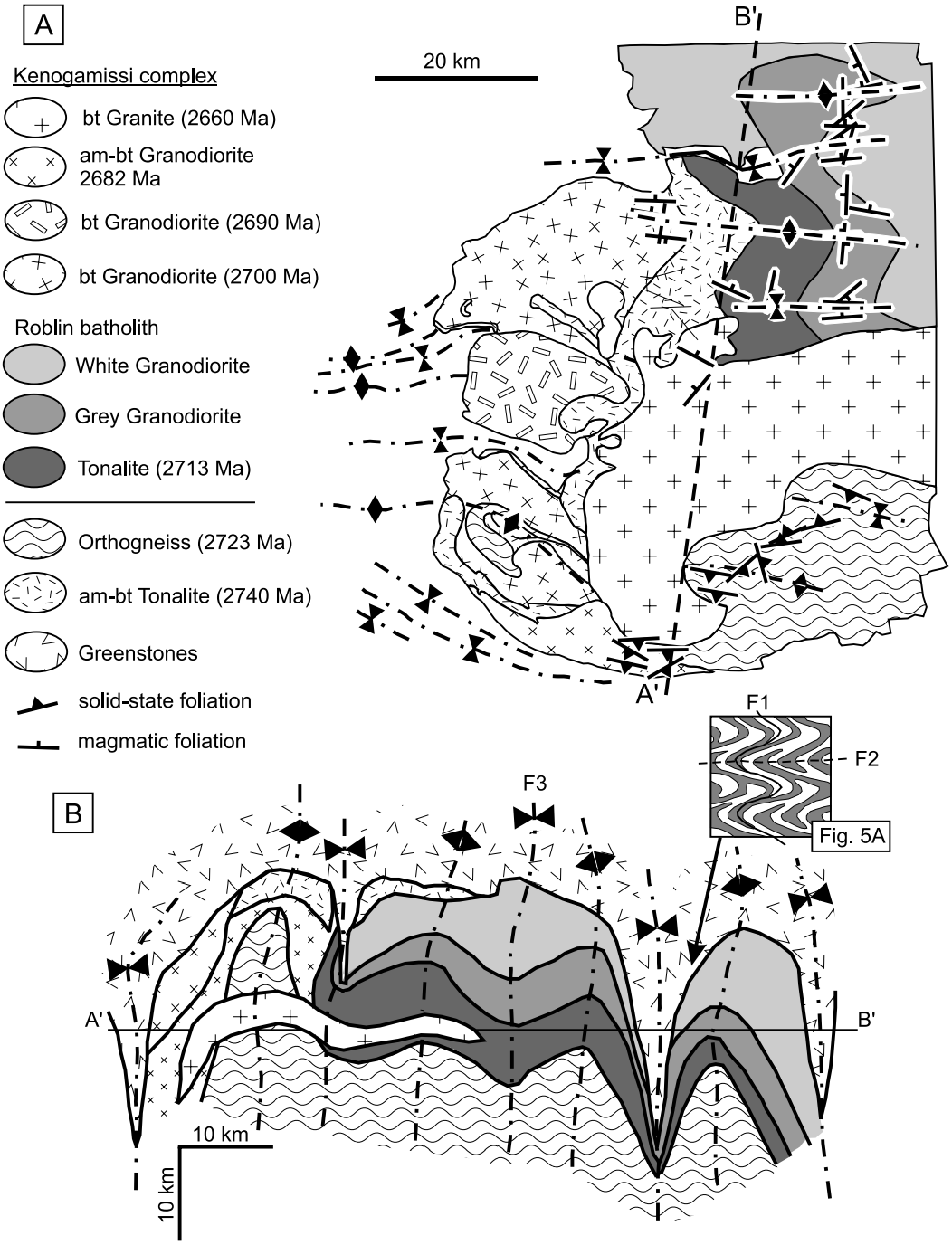

Figure 6 (A) Map of the Kenogamissi complex showing representative measurements of metamorphic foliation in the orthogneiss unit and in deformed rocks near the southern margin of the complex, and magmatic foliations in the Roblin Batholith. (B) Profile through the Kenogamissi complex based on mapping by the present author in the orthogneiss unit and in the Roblin Batholith, and on existing geological maps (Heather 1999). No vertical exaggeration is implied; however, the vertical dimensions of units are approximate. The inset shows the location of Figure 5A and an ideal F3 refold interference pattern. The profile line is shown in Figure 6A.

Figure 5B occurred while the granodiorites were still partially molten, as indicated by the preservation of igneous textures in the rock and also by the presence of the melt remobilisation structures discussed in the next section. Locally, F3 folding also resulted in the formation of an S3 axial planar foliation, recognised in the field by alignments of biotite crystals (Fig. 5C). Petrographic criteria indicate that the S3 foliation in the granodiorites is also a magmatic fabric.

Interpretations regarding the emplacement of the Roblin Batholith and its role in doming of the Kenogamissi complex must account for the observations and structural data in the previous paragraphs. First, the Roblin Batholith was emplaced during the D2 deformation event, which gave rise to the recumbent F2 folds in the orthogneiss and in the greenstones of the deformation aureole. Secondly, during or following emplacement, a horizontal magmatic foliation was developed throughout the batholith. Thirdly, the magmatic fabric was then folded by F3 while the Roblin Batholith was still a crystal mush.

3.4. Melt remobilisation structures

In the orthogneiss unit and in the three units of the Roblin Batholith, outcrop-scale evidence suggests deformation-assisted extraction and remobilisation of magmatic liquids during the F3 folding event. Examples of melt remobilisation structures are shown in Figures 3C, E, F and 5B.

https://doi.org/10.1017/S0263593300001085 Published online by Cambridge University Press

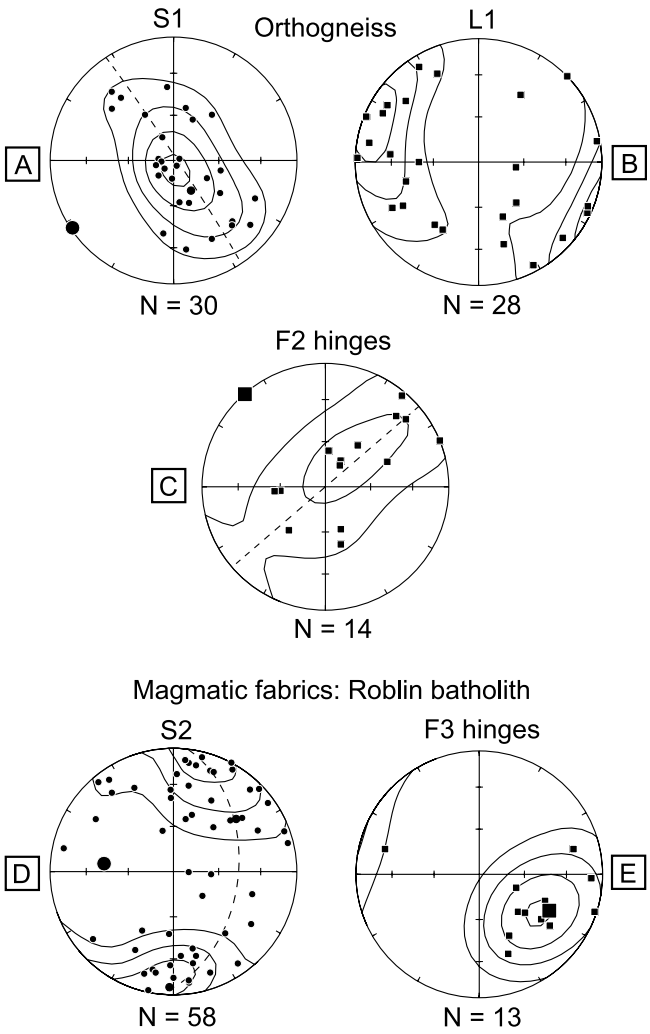

Figure 7 Lower-hemisphere equal-area projections of structural measurements: (A) S1 in the orthogneiss unit. The dashed great circle is the best-fit plane and the large dot indicates the constructed F2 fold axis; (B) L1 in the orthogneiss unit; (C) F2 fold hinges in the orthogneiss unit. The dashed great circle is the best fit plane and the large square indicates the constructed F3 fold axis; (D) S2 magmatic foliation in the Roblin Batholith. The dashed great circle is the best-fit plane and the large dot indicates the constructed F3 fold axis; (E) Field measurements of F3 fold hinges in the Roblin Batholith. The large square indicates the average orientation.

Figure 3C shows an example from the orthogneiss unit, where a leucocratic dyke a few centimetres wide (indicated by the arrow) cross-cuts the folded S2 foliation and the gneissic banding. The photograph is of a vertical outcrop surface. Near the top of the photograph the dyke terminates within one of the leucocratic bands, which is, in essence, a sill. The leucocratic dyke is parallel to, and it is located on, the limb of a mesocopic-scale F3 fold (Fig. 3C). The presence of syn-F3 melt remobilisation structures within the orthogneiss unit raises a question as to the origin of the melt. Detailed petrographic study of the orthogneiss revealed no mineral assemblage that could be attributed to melting reactions, and therefore, the present author rules out the possibility that the rocks could represent migmatites.

According to available geochronological data, the orthogneiss is 10 Ma older than the younger Roblin Batholith. It is unlikely that the vertical dyke in Figure 3C was preserved through the F1 and F2 folding events. It is more likely that the leucocratic dykes and sills in the orthogneiss represent magma that intruded the orthogneiss during emplacement of the tonalite-granodiorite magmas which formed the Roblin Batholith and possibly other, as-yet-unrecognised intrusions.

Figure 3 parts E, F are photographs of an horizontal outcrop surface and they show a similar melt remobilisation structure within the tonalite unit of the Roblin Batholith. There, a leucocratic dyke is in petrographic continuity with S2-parallel leucocratic bands of the same composition within the tonalite. The dyke is parallel to and situated on the limb of an F3 fold. The interpretation is that differentiated magmatic liquid formed narrow bands parallel to S3, and that the liquid was extracted and remobilised into dykes which formed on the sheared limbs of upright F3 folds, as in the outcrop depicted in Figure 3C.

Figure 5B corresponds to a dipping outcrop surface (45° dip angle) in the Roblin Batholith where the grey and white granodiorites are interlayered. The S2 foliation defined by K-feldspar phenocrysts is parallel to the compositional banding. A leucocratic dyke (indicated by the arrow) is parallel to and situated on the limb of an F3 fold of the S2 magmatic foliation and of the compositional banding. The compositional layers in the granodiorite do not match up across the dyke, indicating that the dyke was emplaced within a magmatic shear zone that corresponds to the sheared limb of the F3 fold.

4. Discussion

The present paper provides an overview of the structural geology and the structural evolution of the Kenogamissi complex, a large granitoid-gneiss complex that crops out within greenschist-grade supracrustal assemblages of the Late Archaean Abitibi Subprovince. The study has concentrated on the marginal greenstones in the deformation aureole that surrounds the Kenogamissi complex, on the orthogneiss unit that crops out in the southern part of the Kenogamissi complex and on the newly defined Roblin Batholith that makes up much of its northern part. Figure 8 summarises the interpreted history of deformation and batholith emplacement within the study area, from ca. 2720 through 2700 Ma.

From the profile in Figure 6B, the original prefolding dimensions of the Roblin Batholith are estimated to be at least 80 km in horizontal dimension and about 10 km in thickness. With regards to the vertical thickness of the batholith determined from the profile, it should be noted that the upper margin of the batholith was projected tens of kilometres along periclinal (doubly plunging) fold axes through some regions which require further detailed mapping. Therefore, the thickness of the batholith shown in the profile is estimated to be accurate to ± 2 km. Also, the thickness may well have been increased and decreased locally during syncrystallisation F3 folding if magma was squeezed upward into the cores of the F3 folds shown in Figure 6B.

Mapping results and interpretations of field and petrographic observations indicate that the orthogneiss and the Roblin Batholith underwent the regional folding event that deformed the host greenstone terrane. Field observations also indicate that F3 folding was ongoing while the Roblin Batholith was still partially molten, and that folding led to deformation-assisted melt extraction and remobilisation within the orthogneiss and the Roblin Batholith.

In this section, the present author discusses the emplacement of the Kenogamissi complex as a dome that was inflated by the emplacement of the Roblin Batholith, within the folding greenstone belt. The potential petrological significance of the evidence for deformation-assisted melt remobilisation within the Kenogamissi complex is also discussed.

https://doi.org/10.1017/S0263593300001085 Published online by Cambridge University Press

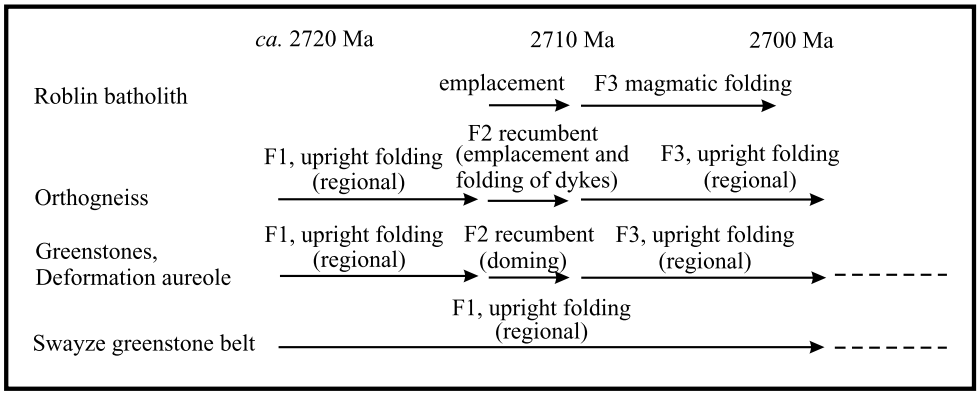

Figure 8 Summary of deformation and batholith emplacement in the study area.

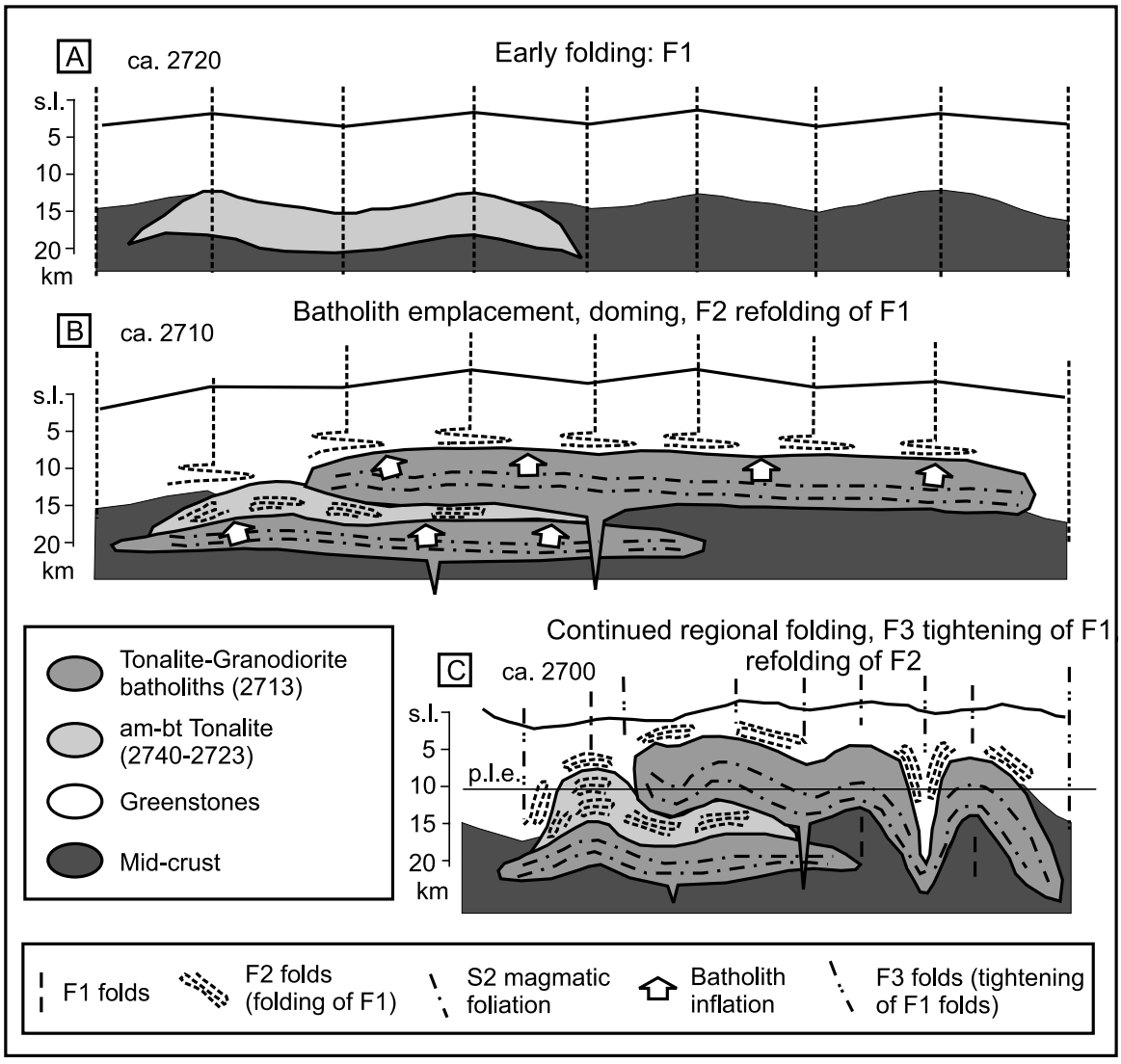

Figure 9 Schematic depiction of the emplacement of the Kenogamissi complex within the greenstones of the Swayze belt by folding, doming and batholith emplacement. See the text for explanations and discussion. Abbreviations: (s.l.) sea level; and (p.l.e.) present level of erosion. The schematic model shown here is approximately to scale.

4.1. Doming and emplacement of the Kenogamissi complex

Based on the mapping, structural analysis and petrographic study, a model is presented for the different stages of evolution of the Kenogamissi complex and the emplacement of the Roblin Batholith. The model, presented schematically in Figure 9, deals only with the evolution of the Kenogamissi complex until ca. 2700 Ma. Other plutonic units, shown in Figure 2, were emplaced later.

The tonalite plutons dated >2720 Ma are here considered to represent magma chambers associated with the metavolcanic units of similar age (Sutcliffe *et al.* 1993). As such, they are interpreted to be tabular intrusions emplaced at the base of the upper crust (Fig. 9A). Doming of the Kenogamissi complex is

https://doi.org/10.1017/S0263593300001085 Published online by Cambridge University Press

shown to have caused severe flattening and recumbent refolding of earlier upright F1 folds in the deformation aureole. Because only one generation of folding is recognised in the Swayze greenstone belt outside of the deformation aureole, the present author interprets that the refolded F1 folds in the deformation aureole represent those regional folds. Upright, regional F1 axial surfaces are shown to deform the greenstones and the early tonalite plutons in Figure 9A.

Emplacement of tonalite-granodiorite batholiths, such as the Roblin Batholith, is shown in Figure 9B. Emplacement and inflation of the batholiths resulted in doming of the Kenogamissi complex and uplift of the overlying greenstones. It also resulted in refolding of the F1 folds in the earlier tonalite plutons, and in the deformation aureole, by recumbent F2 folds (Fig. 9B), giving rise to the refold interference pattern seen in Figure 5A and to recumbent F2 folds in the orthogneiss. At this stage, magmas associated with emplacement of the tonalite-granodiorite batholiths intruded the orthogneiss as dykes and sills. Intrusions of those magmas during doming resulted in recumbent folding of tonalite and granodiorite dykes, giving rise to the heterogeneous compositional makeup of the isoclinally folded orthogneiss. Also at this stage, the magmatic S2 foliation and compositional layering were forming in the Roblin Batholith.

Figure 8C shows F3 folding of the Roblin Batholith, and refolding of F2 folds and of the S2 foliation in the Roblin Batholith. The present author interprets that F3 in the Kenogamissi complex and in its deformation aureole is caused by the continued regional N–S bulk shortening and regional folding which gave rise to the early folds shown in Figure 9A. This interpretation is consistent with F3 having affected the Roblin Batholith while it was still a magma mush, causing remobilisation of fractionated melts, as shown in Figure 5B. It is also consistent with the fact that only one generation of E–W to NW–SE-trending regional folds is documented in the overlying Swayze greenstone belt. Therefore, F3 folding in the Swayze belt in Figure 9C is seen as continued tightening of the regional F1 folds. In other words, F1 regional folding of the Swayze greenstone belt is correlated with both F1 and F3 in the deformation aureole surrounding the Kenogamissi complex. In the Kenogamissi complex and in the deformation aureole, the regional folding event was punctuated by recumbent F2 folding associated with doming.

4.2. Deformation-assisted melt remobilisation

It is widely recognised that deformation-enhanced melt segregation and extraction plays a fundamental role in the chemical differentiation of the continental crust and in the transport of granitic melts from deep zones of partial melting to magma emplacement sites at shallower crustal levels (Clemens & Mawer 1992; Brown 1994; Sawyer 1996; Brown & Solar 1999; Brown 2004). From the observations presented here, it seems that tectonically driven deformation, specifically folding, has played a potentially important role in remobilisation and transport of fractionated liquids within the orthogneiss unit and also within the partially solidified Roblin Batholith. An important interpretation that arises from those observations is that deformation-assisted remobilisation of melts may have been important in the formation of compositional layering (injection of sills, Fig. 3C) and also in the magmatic differentiation of the batholith.

In the examples shown in Figures 3C, E, F and 5B, the leucocratic dykes are located on, and are parallel to, the sheared limbs of F3 folds. In the cases of leucocratic dykes in the Roblin Batholith, the folds are synmagmatic. The present author interprets the melts to have been injected into the deforming orthogneiss unit from the Roblin Batholith or from an underlying, unexposed intrusion of the same age as the Roblin Batholith. At the time of F3 folding, the latest of the injected melts had only partially crystallised and fractionated, such that liquid was available to be remobilised during that folding event (Fig. 3C).

The documented leucocratic dykes are small-scale features, of the order of a few centimetres to 15 cm in thickness. However, their occurrences are widespread and common, suggesting that they may represent a significant remobilisation of magmatic liquid. Also, it cannot be ruled out that similar but larger dykes may remain as yet unidentified.

In the Kenogamissi complex, deformation-assisted remobilisation of magmatic liquids, which potentially contributed to the fractionation of the Roblin Batholith, was the result of tectonic folding of the partially molten Roblin Batholith and of the orthogneiss that contained injected melt. The present author is not aware of melt remobilisation structures of the type described here, located on the sheared limbs of upright magmatic folds, having been previously documented in the literature. Recently published work on the Archaean Woodstock monzogranite (Pilbara Craton) has documented emplacement of leucocratic granitic magmas into magmatic shear zones which formed within the folding, partially molten monzogranite (Pawley & Collins 2002; Pawley *et al*. 2002). In that case, the magmatic shear zones cross-cut magmatic fold limbs in the host pluton and they are interpreted to have formed in response to a bulk dextral shearing of the crystallising monzogranite. The work of Pawley and colleagues, together with the results presented here, indicate that deformation-assisted extraction and remobilisation of fractionated melts within crystallising intrusions may be an important, although previously unrecognised process in syntectonic plutons and batholiths. As seen in Figure 3C, it can lead to the formation of magmatic compositional layering (sills). It may also result in significant redistribution of mass and affect chemical differentiation histories of the deforming magma bodies.

Understanding the full significance of the deformation-enhanced melt remobilisation and transport within the Kenogamissi complex will require further, more detailed structural, microstructural and petrological studies. In particular, it will be important to discover whether the types of melt remobilisation structures documented here caused the redistribution of large volumes of melt, and at what length and time scale the melt redistribution was efficient. However, it is reasonable to speculate that deformation-assisted extraction and redistribution of melt within mushy plutons which are subjected to regional tectonic deformation, in particular folding, may represent a previously unrecognised though important mechanism for the magmatic differentiation of syntectonic plutons and batholiths.

It will also be important to better understand the significance of the localisation of melt remobilisation structures, such as the dykes documented here, on the limbs of folds. In magmatic shear zones it is expected that mechanical interactions of rigid solid phases will result in localised dilatation, as is the case in shear zones developed during flow of unconsolidated granular materials such as sand (Mandl *et al*. 1977; Du Bernard *et al*. 2002). It has also been suggested that shear localisation and increased dilatancy may occur in deforming, crystallising granitic magmas and lead to melt segregation (Vigneresse & Tikoff 1999). That is in agreement with the structures documented in the present paper. It is speculated that dilatation caused by shearing of crystal mush on the limbs of magmatic folds in the Roblin Batholith led to the migration of melts to the fold limbs and the formation of the leucocratic dykes.

5. Conclusions

Mapping, structural analysis and petrographic study of the orthogneiss unit and the three units of the Roblin Batholith provide insights into the history of the doming and emplacement of the Late Archaean Kenogamissi complex into the greenstones of the Swayze greenstone belt in the Abitibi Subprovince, Ontario. Doming resulted from the emplacement and inflation of tonalite-granodiorite batholiths, such as the Roblin Batholith, in the lower stratigraphic levels of the greenstone belt and possibly in the underlying crust. Doming led to the horizontal flattening of earlier tonalite plutons and of the greenstones within the deformation aureole that surrounds the Kenogamissi complex, and the formation of recumbent F2 folds. The recumbent, doming-related folds refolded earlier, regional E–W to NW–SE-trending F1 regional folds in the earlier plutons and in the deformation aureole. Injection of magmas related to the tonalite-granodiorite batholiths into the earlier plutons and concomitant flattening caused by doming resulted in the heterogeneous compositional layering in the isoclinally (F2) folded orthogneiss unit.

The doming and related recumbent folding punctuated one long-lived regional folding event that continued during and after doming, folding the orthogneiss and the Roblin Batholith while the latter remained a magma mush, forming F3 folds in the orthogneiss, the Roblin Batholith and in the deformation aureole. Effectively, F1 folds and F3 folds within the deformation aureole of the Kenogamissi complex both correlate with the one generation of regional folds in the overlying and surrounding greenstone belt.

The tectonic deformation and folding of the Kenogamissi complex resulted in syntectonic extraction and redistribution of fractionated melts within the deforming Roblin Batholith magma mush and within the orthogneiss. Magma was extracted and remobilised into dykes which formed on the sheared limbs of magmatic folds. The concentration of melt on the limbs of magmatic folds, which led to the formation of the dykes, was probably allowed by dilatancy caused by shearing of the crystal-liquid suspension (magma mush) on the fold limbs.

Further structural and petrological study will be required to evaluate the length and time scales over which deformation-assisted melt remobilisation was efficient within the Kenogamissi complex. However, it is suggested that deformation-assisted melt remobilisation and redistribution may prove to be an important process in the magmatic differentiation histories of syntectonic plutons and batholiths.

6. Acknowledgements

This research was funded by a Natural Sciences and Engineering Research Council of Canada Discovery Grant. Insightful comments and suggestions by journal reviewers R. Anma and R. Weinberg were very helpful in improving the final manuscript. I also wish to thank M. Brown for discussions which focused my ideas and improved my interpretations. The organisers of the Hutton V Symposium on Granites and Related Rocks in Toyohashi, Japan, and the editors of this special issue are also thanked for the opportunity to present this work at the symposium and to publish it in the journal.

7. References

Ayer, J. A., Amelin, Y., Corfu, F., Kamo, S. L., Ketchum, J., Kwok, K. & Trowell, N. 2002a. Evolution of the southern Abitibi greenstone belt based on U-Pb geochronology: authochthonous volcanic construction followed by plutonism, regional deformation and sedimentation. *Precambrian Research* **115**, 63–95.

Ayer, J. A., Ketchum, J. W. F. & Trowell, N. F. 2002b. New geochronological and neodymium isotopic results from the Abitibi greenstone belt, with emphasis on the timing and the tectonic implications of Neoarchean sedimentation and volcanism. Summary of field work and other activities. *Ontario Geological Survey, Open File Report 6100*, pp. 5.1–5.16.

Becker, J. K. & Benn, K. 2003. The Neoarchean Rice Lake batholith and its place in the tectonomagmatic evolution of the Swayze and Abitibi granite-greenstone belts, northeastern *Ontario. Ontario Geological Survey, Open File Report 6105*, p. 42.

Bouchez, J. L., Gleizes, G., Djouadi, T. & Rochette, P. 1990. Microstructure and magnetic susceptibility applied to emplacement kinematics of granites: the example of the Foix pluton (French Pyrenees). *Tectonophysics* **184**, 157–71.

Brown, M. 1994. The generation, segregation, ascent and emplacement of granite magma: the migmatite-to-crustally-derived granite connection in thickened orogens. *Earth-Science Reviews* **36**, 83–130.

Brown, M. 2004. The mechanism of melt extraction from lower continental crust of orogens. *Transactions of the Royal Society of Edinburgh: Earth Sciences* **95**, 35–48.

Brown, M. & Solar, G. S. 1999. The mechanism of ascent and emplacement of granite magma during transpression: a syntectonic granite paradigm. *Tectonophysics* **312**, 1–33.

Clemens, J. D. & Mawer, C. K. 1992. Granitic magma transport by fracture propogation. *Tectonophysics* **204**, 339–60.

Du Bernard, X., Eichhubl, P. & Aydin, A. 2002. Dilation bands: a new form of localized failure in granular media. *Geophysical Research Letters* **29**, doi:10.1029/2002GL015966.

Heather, K. B. 1999. *Geology of the Swayze greenstone belt, Ontario. Open File 3384*. Ottawa: Geological Survey of Canada.

Mandl, G., de Jong, L. N. J. & Maltha, A. 1977. Shear zones in granular material. *Rock Mechanics* **9**, 95–144.

Nitescu, B. & Halls, H. C. 2002. A gravity profile across southern Saganash Lake fault: implications for the origin of the Kapuskasing structural zone. *Canadian Journal of Earth Sciences* **39**, 469–80.

Paterson, S. R., Vernon, R. H. & Tobisch, O. T. 1989. A review of criteria for the identification of magmatic and tectonic foliations in granitoids. *Journal of Structural Geology* **11**, 349–63.

Pawley, M. J., Collins, W. J. & Van Kranendonk, M. J. 2002. Origin of fine-scale sheeted granites by incremental injection of magma into active shear zones: examples from the Pilbara Craton, NW Australia. *Lithos* **61**, 127–39.

Pawley, M. J. & Collins, W. J. 2002. The development of contrasting structures during the cooling and crystallisation of a synkinematic pluton. *Journal of Structural Geology* **24**, 469–83.

Percival, J. 1988. Deep geology out in the open. *Nature* **335**, 671.

Ramsay, J. G. 1967. *Folding and Fracturing of Rocks*. New York, NY: McGraw-Hill Book Company.

Sawyer, E. W. 1996. Melt segregation and magma flow in migmatites: implications for the generation of granite magmas. *Transactions of the Royal Society of Edinburgh: Earth Sciences* **87**, 85–94.

Sutcliffe, R. H., Barrie, C. T., Burrows, D. R. & Beakhouse, G. P. 1993. Plutonism in the southern Abitibi Subprovince: a tectonic and petrogenetic framework. *Economic Geology* **88**, 1359–75.

Thiessen, R. 1986. Two-dimensional refold interference patterns. *Journal of Structural Geology* **8**, 563–73.

Vernon, R. H. 2000. Review of microstructural evidence of magmatic and solid-state flow. *Electronic Geosciences* **5**. (www documents.) URL http://link.springer-ny.com/link/service/journals/10069/bibs/0005001/00050002.htm

Vigneresse, J. L. & Tikoff, B. 1999. Strain partitioning during partial melting and crystallizing felsic magmas. *Tectonophysics* **312**, 117–32.

KEITH BENN, Ottawa-Carleton Geoscience Centre and Department of Earth Sciences, University of Ottawa, Ottawa, Ontario K1N6N5, Canada.
e-mail: kbenn@uottawa.ca

MS received 20 October 2003. Accepted for publication 14 September 2004.